Journal of
Marine Science and Engineering

MDPI

Article

Annual and Seasonal Variation of the Ocean Thermal Resources off the Mexican Coast

Carlos Melecio Carmona-Cedillo [1], Armando Trasviña-Castro [2], Valeria Chávez [1,*] and Rodolfo Silva [1,*]

[1] Instituto de Ingeniería, Universidad Nacional Autónoma de México, Mexico City 04510, Mexico; mitla@yahoo.com
[2] Centro de Investigación Científica y de Educación Superior de Ensenada, Unidad La Paz, La Paz 23050, Baja California Sur, Mexico; trasvi@cicese.mx
* Correspondence: vchavezc@iingen.unam.mx (V.C.); rsilvac@iingen.unam.mx (R.S.)

Abstract: A large amount of thermal energy is stored in the oceans between the tropics, available for conversion into electrical energy using OTEC technology. The aim of this study was to determine the annual and seasonal variability of the oceanic thermal resource in Mexico. Using the WOA18 database, we mapped surface temperature at a 10 m depth, deep cold water (<5 °C), vertical temperature difference (18 and 20 °C), and temperature anomalies. From the results, four areas were analyzed as being suitable for the installation of OTEC technology: Pacific (A), Los Cabos (B), Caribbean (C), and Gulf of Mexico (G). The optimal thermal resource (≥20 °C) was found between a 400 and 1000 m depth in all seasons in A and C, in spring, summer, and autumn in G, and only in summer and autumn in B. The suboptimal thermal resource (between 18 and 20 °C) was present between 400 and 800 m in all seasons in A, C, and G, and in summer and autumn in B. These results provide new information of utmost importance for future location and design considerations of OTEC plants on Mexican coasts, and the methodology can be used in other areas where there is a lack of field data and the development of OTEC technology is being considered.

Keywords: thermal energy; OTEC; oceanic vertical temperature difference; anomaly; WOA18 database

check for updates

Citation: Carmona-Cedillo, C.M.; Trasviña-Castro, A.; Chávez, V.; Silva, R. Annual and Seasonal Variation of the Ocean Thermal Resources off the Mexican Coast. *J. Mar. Sci. Eng.* **2024**, *12*, 1160. https://doi.org/10.3390/jmse12071160

Academic Editor: Decheng Wan

Received: 7 June 2024
Revised: 28 June 2024
Accepted: 6 July 2024
Published: 10 July 2024

Copyright: © 2024 by the authors. Licensee MDPI, Basel, Switzerland. This article is an open access article distributed under the terms and conditions of the Creative Commons Attribution (CC BY) license (https://creativecommons.org/licenses/by/4.0/).

1. Introduction

Of all the sustainable sources of marine energy available, the harnessing of power using Ocean Thermal Energy Conversion (OTEC) is one of the most feasible for Mexican waters. When the temperature gradient is substantial between the warmer surface of the sea and the colder water at depth, this difference can be harnessed to power turbines, thus producing electricity. The historical development of this idea can be found in the pioneering literature on the subject (e.g., Anderson [1] and Uehara [2]). OTEC technology requires huge quantities of hot and cold seawater and a temperature gradient of more than 20 °C between hot and cold water to obtain the lowest theoretical maximum thermal efficiency (3–10%) of the heat engine [3,4]. The availability of the thermal resource (temperature difference) based on the availability and accessibility of hot surface water (heat source) and deep cold water (heat sink) is essential for the productivity and economic profitability of an OTEC plant [5,6].

On a global scale, the available thermal resource is estimated at around 30 TW, and it is believed that the extraction of 7 TW would have a negligible impact on the thermal structure of the ocean [7]. Theoretically, the resource is available between 0 and 23° latitude in the northern hemisphere [8]. But the question is, in reality, how much of the thermal resource available globally is within reach, practically, for use in OTEC plants?

Specific studies on the availability of the temperature difference between surface water and water at greater depths have been carried out in the Caribbean Sea [9,10], in Cuba [3], Puerto Rico [11], and the Virgin Islands [12]; Atlantic Ocean, in the Gulf Stream [13,14], Florida [15,16], Gulf of Mexico [17], Brazil [18], and the Ivory Coast [19]; in the Pacific

Ocean [20,21], in Dampier Land [22], Japan [2,23], Hawaii [24,25], Guam [26], Manila [23,27], Kiribati [28], and Malaysia [29], and in the Indian Ocean, in Sri Lanka [30], Mombasa [31], Jakarta [32], and around Mexico [33–40]. In addition, to test the feasibility of this technology, small OTEC plants have been constructed at Nauru, Tokunoshima, and Imari [23,24,41].

The available ocean thermal energy has natural variability due to oceanographic and meteorological processes, including environmental disturbances, or even unpredictable extreme events. Therefore, it is advisable to use long-term temperature data to determine operating conditions and to allow the identification of extreme events that might occur during the operation of an OTEC plant. In order to fill this gap in Mexico, this research sought to determine the baseline, or reference point, of the thermal resource (optimal and suboptimal) and determine the coastal areas where it is available and accessible in Mexican waters and in the seasonal cycle. The temperature variation in Mexican oceanic waters was determined using the World Ocean Data (WOA) [42].

Section 2 of this work presents the study area and describes the methodology followed to determine the thermal resource in Mexico. Section 3 shows the results of the spatial–time thermal resource distribution in annual and seasonal cycles, analyzing the optimal (≥20 °C) and suboptimal (between 18 and 20 °C) vertical temperature difference for OTEC deployment. Section 4 offers a discussion and, finally, in Section 5 the conclusions of this work are presented, highlighting the relevance of this study for the design of any OTEC plant and the selection of installation sites in Mexico.

2. Methods

2.1. Study Area

Figure 1 shows physical characteristics of the Mexican coasts relevant to their suitability for OTEC technology, in particular, the configuration of the sea bottom. The oceanic depths shown in Figure 1 were taken from the General Bathymetric Chart of the Oceans (GEBCO) database [43].

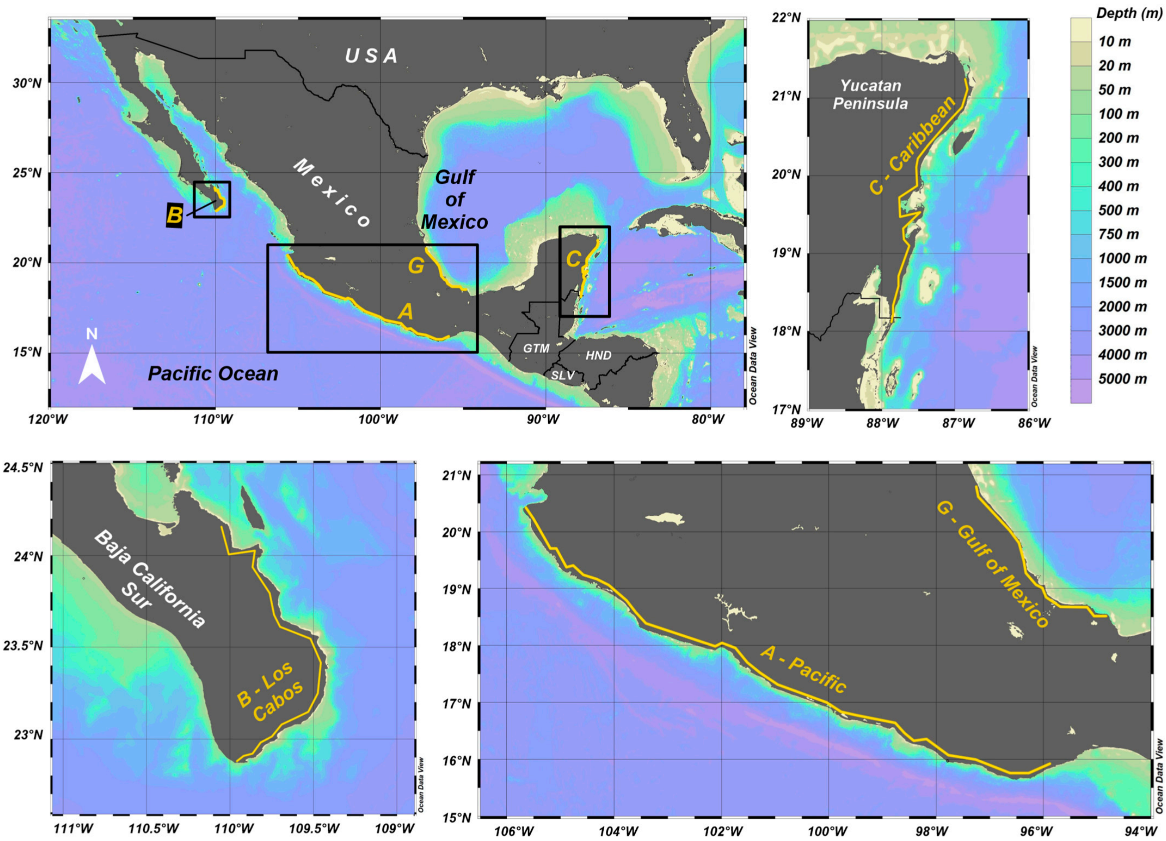

Figure 1. Study area. The four coastal areas shown are where the continental platform is near the coastline (yellow lines, A, B, C, and G). Bathymetry from GEBCO.

The four coastal zones, marked as A, B, C, and G in Figure 1, are where there is deep water (<1000 m) close to the coast, and include sites mentioned by Alatorre et al. [33]. These are: Pacific (A), on the Pacific coast, from 15.7 (Puerto Angel) to 20.4° N (Cabo Corrientes); Los Cabos (B), off the Baja California Peninsula coast, from 22.9 (Cabo San Lucas) to 24.2° N (Isla Cerralvo); Caribbean (C), on the Mexican Caribbean coast, from 18.3 (Xcalak) to 20.8° N (Puerto Morelos), and the Gulf of Mexico (G), on the Gulf of Mexico coast, from 18.1 (Coatzacoalcos) to 20.5° N (Tecolutla).

2.2. Ocean Temperature Estimation

For efficient operation, an OTEC plant needs an optimal vertical temperature difference (VTD) of $\geq$20 °C, with a tolerance of 2 °C, representing the suboptimal temperature difference of 18 $\leq$ VTD < 20 °C. Therefore, the optimal and suboptimal sea surface temperatures of interest were 25 and 23 °C, respectively, considering a cold water temperature of 5 °C [44]. In Mexico, there is a database published by the Sistema de Vigilancia Oceánica por Satélite (SATMO), which is part of the Sistema de Información y Análisis Marino Costero (SIMAR) that has daily data since 1 June 2002, with a spatial resolution of 0.01 degrees [45]. García-Huante et al. [34] made a comparison of the SIMAR database and the World Ocean Atlas [42] and measured data, finding that for weekly temperature averages, both databases were reliable, as the errors were around less than one degree centigrade. For this reason, we decided to use a global database.

We analyzed the World Ocean Atlas [42] data for a 0.25° temperature grid, at 102 standard depth levels, from the sea surface to a depth of 5500 m. The temperatures studied were the average of six decadal periods, from 1955 to 2017, using the annual and seasonal (three months) average temperature data available for each of the 7656 WOA stations. The seasons were defined as: winter (January–February–March), spring (April–May–June), summer (July–August–September), and autumn (October–November–December) [46–48]. In addition, the seasonal ocean temperature difference between the surface and particular depths was used [42].

The vertical temperature difference (VTD) was calculated using the long-term mean sea surface temperatures at a 10 m depth (SST10) minus the deep-water temperatures (DWT) at depths of 400, 500, 600, 700, 800, 900, and 1000 m by Equation (1):

$$\text{VTD} = \text{SST10} - \text{DWT} \tag{1}$$

The temperature at a 10 m depth (SST10) was chosen as the reference for the determination of the VTD, as this avoids any possible surface diurnal variations, or other sources of variability from wind- and wave-induced turbulence and air–sea heat fluxes.

Finally, a temperature anomaly was estimated by subtracting the annual climatology (1955–2017) from the seasonal climatological temperature.

3. Results

Table 1 shows the seasonal depths of the 20 °C (optimal) and 18 °C (suboptimal) VTD isotherms in the four coastal areas of interest. It was observed that the seasonal VTD of the optimal resource was absent in winter off Los Cabos (B) and in the Gulf of Mexico (G). The deepest 20 °C VTD isotherm (>1000 m) was found off Los Cabos in spring, while the shallowest (370–420 m) was observed in the Pacific in summer. On the other hand, the deepest 18 °C VTD isotherm (>1000 m depth) was found off Los Cabos in winter and spring, while the shallowest (250–280 m depth) occurred in the Pacific in summer.

The following sections present, in detail, the data used to determine the depths of the 20 and 18 °C VTD isotherms (Table 1).

Table 1. Depth ranges of the 20 and 18 °C VTD isotherms near the analyzed coastal zones.

Coast	Depth of the 20 °C VTD Isotherm (m)				Depth of the 18 °C VTD Isotherm (m)			
	Winter	Spring	Summer	Autumn	Winter	Spring	Summer	Autumn
Pacific (A)	550–1000	450–800	370–420	400–500	400–600	300–550	250–280	300–400
Los Cabos (B)	–	>1000	500–600	600–700	>1000	>1000	360–400	460–500
Caribbean (C)	700–800	550–700	500–600	550–600	500–600	450–500	400–470	450–500
Gulf of Mexico (G)	–	640–700	440–500	600–650	750–875	460–500	320–380	400–450

3.1. Mean Annual Temperature

The horizontal pattern of mean annual sea surface temperatures at 10 m (SST10) displayed an inverse latitudinal relationship, whereby the variable increased toward lower latitudes (Figure 2a). This pattern was seen around Mexico: from 16 (33° N) to 29 °C (14.8° N) in the Pacific Ocean, from 23 (30° N) to 26.8 °C (19° N) in the Gulf of Mexico, and from 27 (22° N) to 28 °C (18.6° N) in the Caribbean Sea. The SST10 for the four coastal areas was always above 25 °C. For instance, in the Pacific littoral (A), it varied from 26.5 (20.6° N) to 29 °C (16° N), in the Caribbean (C) from 27.4 (21° N) to 27.8 °C (18.4° N), and in the Gulf of Mexico (G) from 26 (20.5° N) to 26.5 °C (18.4° N), with the only exception off Los Cabos (B), where the SST10 varied from 23 to 24 °C.

The contour map of the mean annual 5 °C isotherm is shown in Figure 2b. Cold water occurred at a 860–865 m depth off Los Cabos (line marked B), along the Pacific (line A) it was at 880 (20.3° N) and 912 m (15.4° N), in the Gulf of Mexico (line G) between 914 (19.1° N) and 950 m (20.6° N), and in the Caribbean (line C) between 950 (18.1° N) and 1000 m (20.6° N).

Near the coast, the suboptimal warm water isotherm (23 °C; Figure 2c) was seen between 20 and 25 m depths at Los Cabos (line B), between 42 (20.3° N) and 51.5 m (15.6° N) depths in the Pacific (line A), from 49 (18.6° N) to 52 m (20.6° N) depths in the Gulf of Mexico (line G), and from 122 (20.8° N) to 144 m (19.1° N) depths in the Caribbean (line C).

There was no optimal 25 °C isotherm (Figure 2d) near Los Cabos (line B) at the sea surface. However, it was present in the Pacific (line A) at 29 (20.3° N) and 42 m (16.1° N) depths, in the Gulf of Mexico (line G) between 25 (18.3° N) and 30 m (20.4° N), and in the Caribbean (line C) from 90 (20° N) to 105 m (18.3° N).

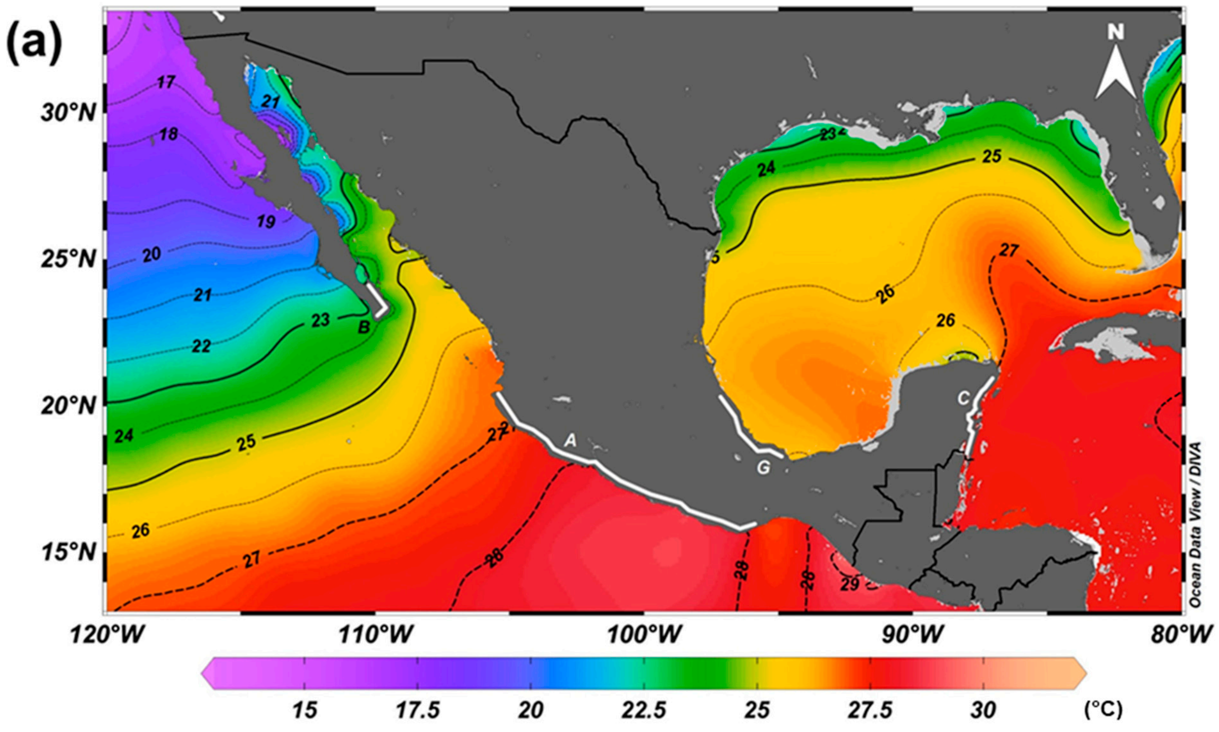

Figure 2. *Cont.*

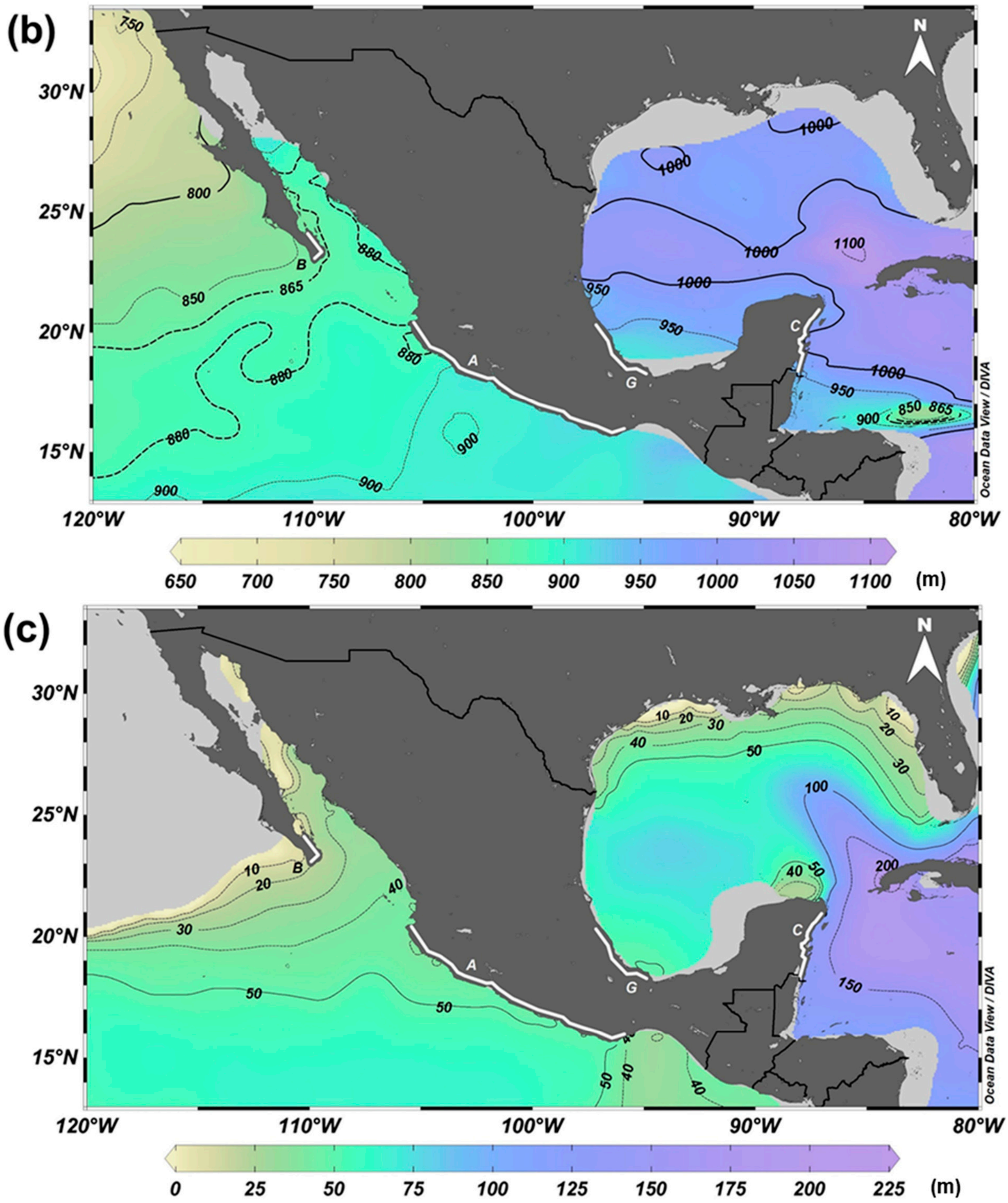

Figure 2. *Cont.*

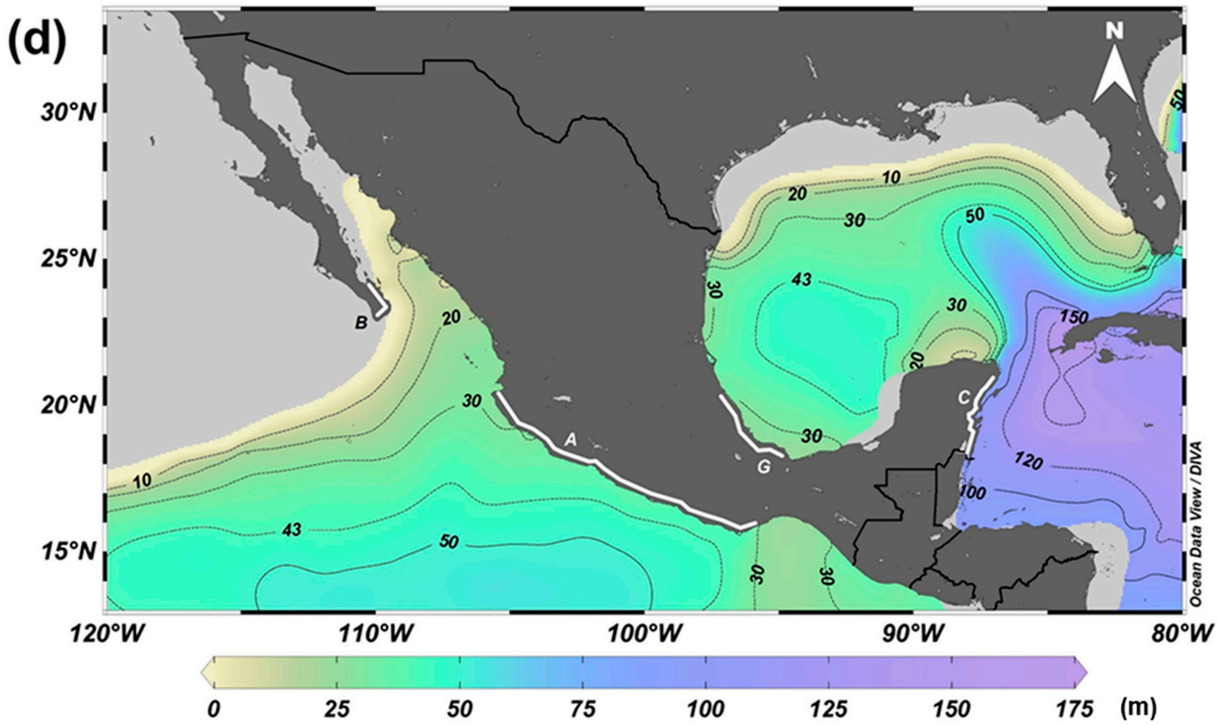

Figure 2. (**a**) Annual mean sea temperature at a 10 m depth (SST10). (**b**) Deep cold water (5 °C isotherm) depth, (**c**) suboptimal warm water (23 °C isotherm) depth, and (**d**) optimal warm water (25 °C isotherm) depth. Areas of interest shown: (A) Pacific, (B) Los Cabos, (C) Caribbean, and (G) the Gulf of Mexico. WOA18 data.

The annual average temperature serves to show the presence of the resource almost everywhere near to the Mexican coast, except off the west coast of the Yucatán Peninsula, due to the broad continental shelf found there. Information about the seasonal variability of temperature anomalies is presented in Section 3.3.

3.2. Annual Vertical Temperature Difference (VTD)

VTDs of over 20 °C are considered optimal for energy generation using the OTEC process. They were found in the four coastlines of interest at shallow depths, at around a 700 m depth. Only around Los Cabos were temperatures differences (18 ≤ VTD < 20 °C) suboptimal (Figure 3a).

Figure 3b,c present the depth of 18 and 20 °C VTDs, respectively, indicating the distribution of sites where both the surface warm water (SST10) and deep cold water are ideal for the deployment of an OTEC plant.

In Figure 3c, the depth of the annual 20 °C VTD isotherm near the coast is seen between 440 (16.1° N) and 600 m (20.6° N) in the Pacific coast (line A), in the Gulf of Mexico (line G) between 650 (19.1° N) and 700 m (20.9° N), and in the Caribbean (line C) between 580 (18.4° N) and 650 m (20.9° N). Only off Los Cabos (line B) was this optimal VTD over 1000 m in depth.

The depth of the suboptimal annual VTD 18 °C isotherm is presented in Figure 3b. It is located off the Pacific coast between 321 (16.1° N) and 431 m (20.4° N) depths (line A), between 480 (18.9° N) and 485 m (20.4° N) depths in the Gulf of Mexico (line G), from 460 m (18.4° N) to 500 m (20.9° N) depths in the Caribbean (line C), and between 600 to 700 m depths off Los Cabos (line B).

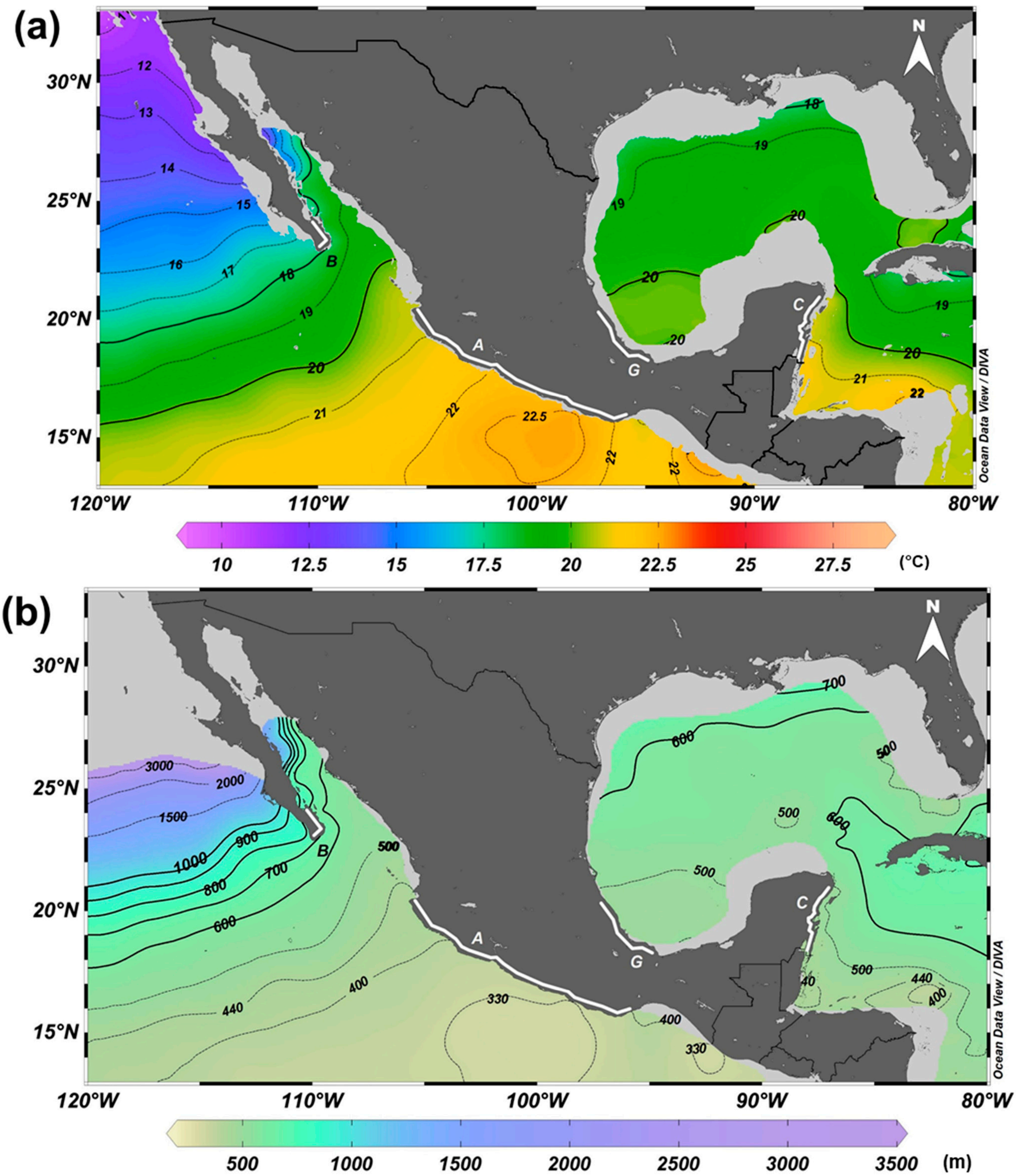

Figure 3. *Cont.*

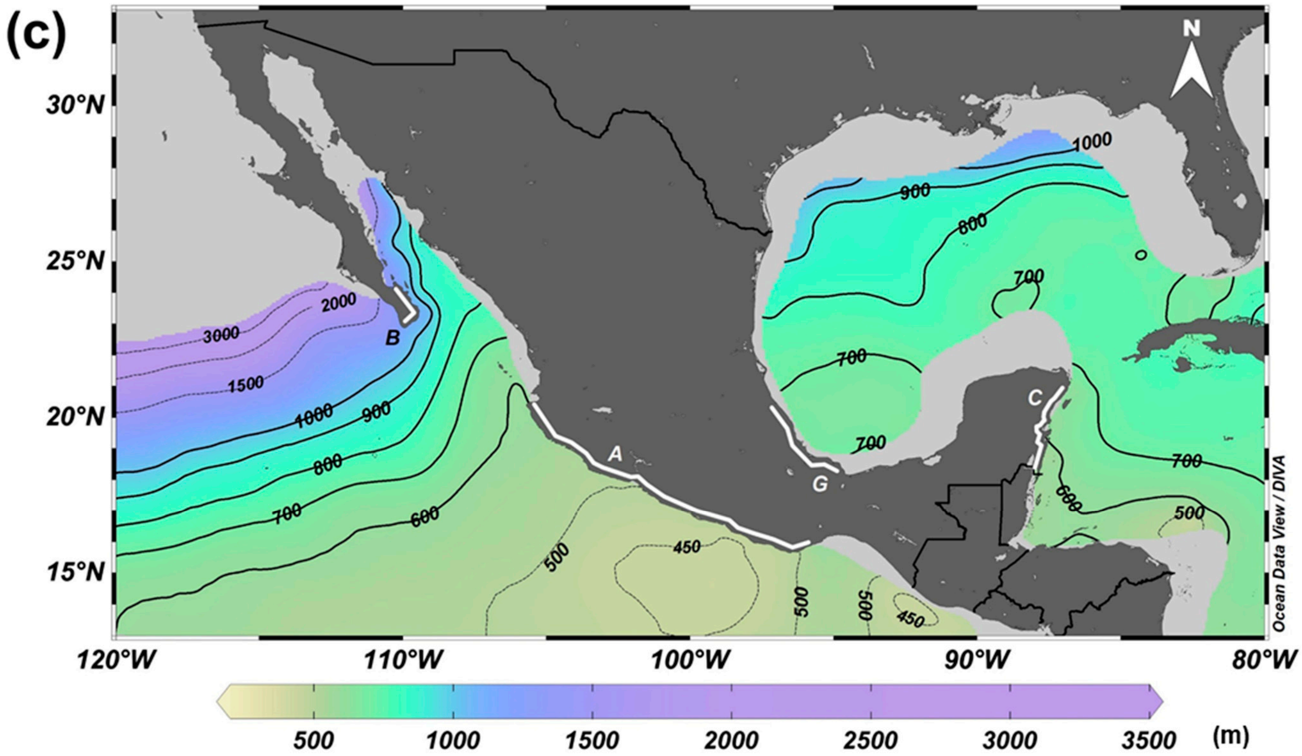

Figure 3. (**a**) Annual VTD at a 700 m depth (estimated from WOA18 data using Equation (1)). (**b**) Suboptimal VTD (18 °C isothermal) depth and (**c**) optimal VTD (20 °C isothermal) depth. Areas of interest shown: (A) Pacific, (B) Los Cabos, (C) Caribbean, and (G) the Gulf of Mexico. WOA18 data.

3.3. Seasonal Thermal Resource

3.3.1. Seasonality of Sea Surface Temperature at 10 m Depth (SST10)

Sea surface temperature off the coast of Mexico exhibits a seasonal variability affected by two main processes: the currents and the solar radiation cycle. The west coast of Baja California cools down in the winter (Figure 4a) and spring (Figure 4b), and SST10 remains below 25 °C along most of the coast. This is due to the presence of the California Current (CC). Later in the year, the CC moves further from the coast, allowing warmer tropical waters to move into this area (Figure 4c,d), although at SST10 the water remains cool, with the exception of the extreme south, where SST10 values fall below 25 °C. At the entrance to the Gulf of California, there is a great seasonal variability, with cooler waters in the winter and very warm waters in the summer, associated with the poleward advance of tropical waters. Here, SST10 values in the winter are similar to the west coast, but in summer, they rise to 28 °C or more. The southern Pacific and the Caribbean coast both remain warm throughout the year with SST10 above 25 °C almost everywhere, except around 20 N in the Pacific. Finally, the Gulf of Mexico coastline exhibits a pronounced seasonal variability with well-defined changes every season (Figure 4). This is why SST10 remains below 25 °C throughout the winter.

Summarizing, SST10 remains $\geq$25 °C all year long in most of the Pacific (line A) and the Caribbean (line C). In the Gulf of Mexico (line G), the SST10 falls below 25 °C in the winter. In the vicinity of Los Cabos (line B), SST10 below 25 °C occurs during winter and spring.

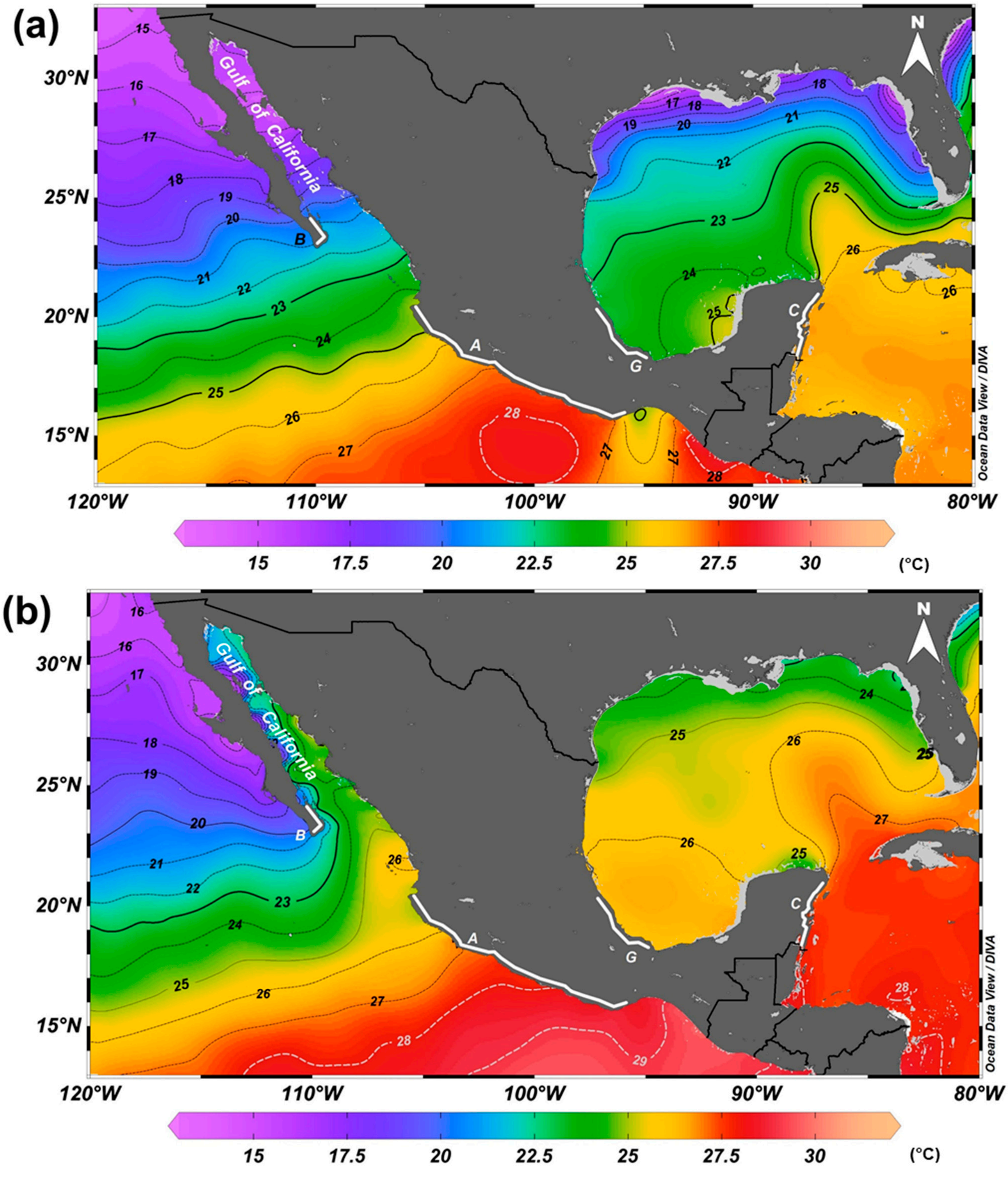

Figure 4. *Cont*.

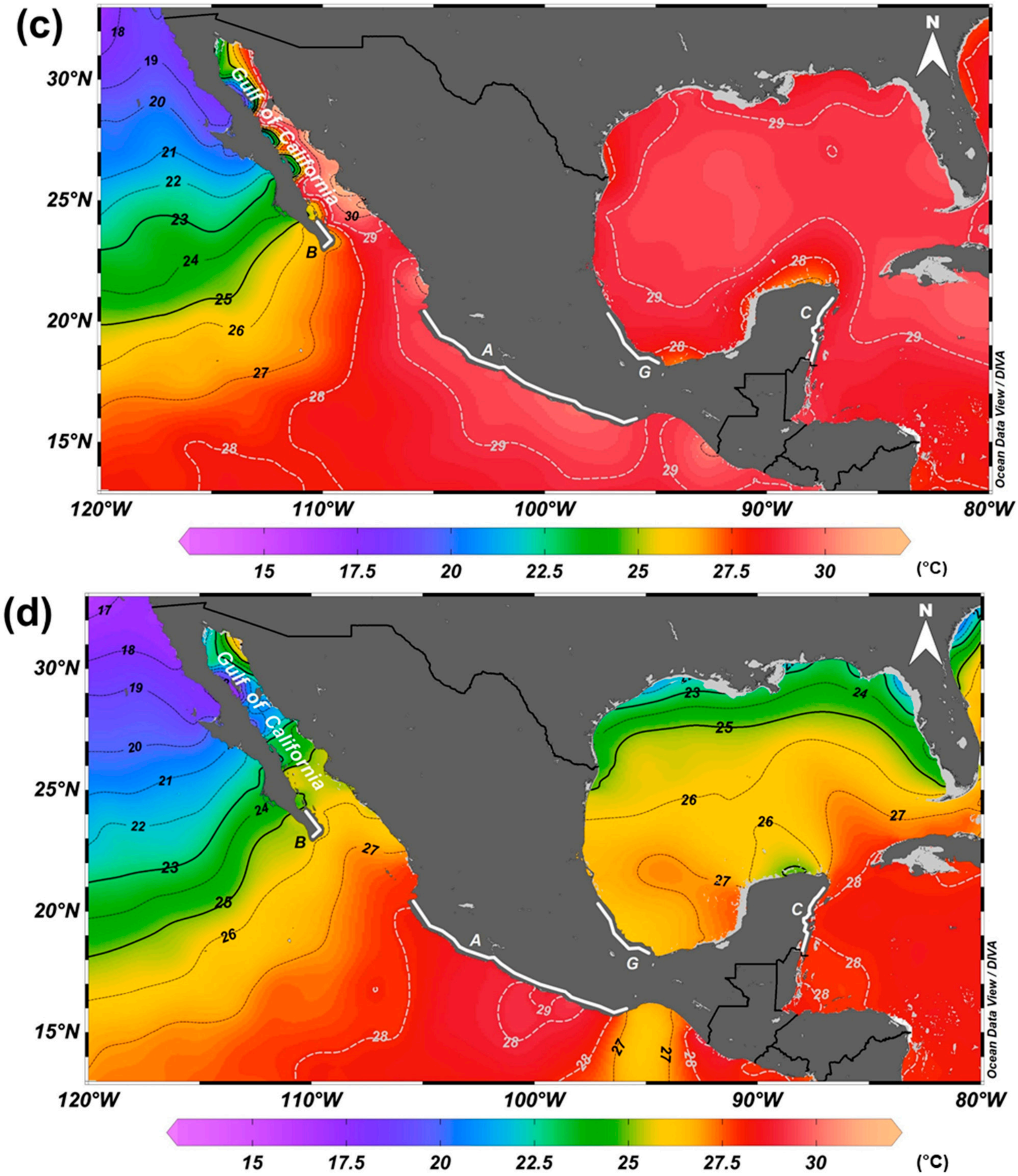

Figure 4. Seasonal ocean temperature at a 10 m depth: (**a**) winter, (**b**) spring, (**c**) summer, and (**d**) autumn. The 23 and 25 °C isotherms (black bold lines) identify hot water that could be useful for OTEC near the coast at Los Cabos (line B), in the Pacific (line A), on the Gulf of Mexico (line G), and in the Caribbean (line C). WOA18 Data.

3.3.2. Seasonality of SST10 Temperature Anomalies

Figure 5 and Table 2 present the SST10 temperature anomalies. The anomalies are relative to the annual mean SST10 from 1955 to 2017.

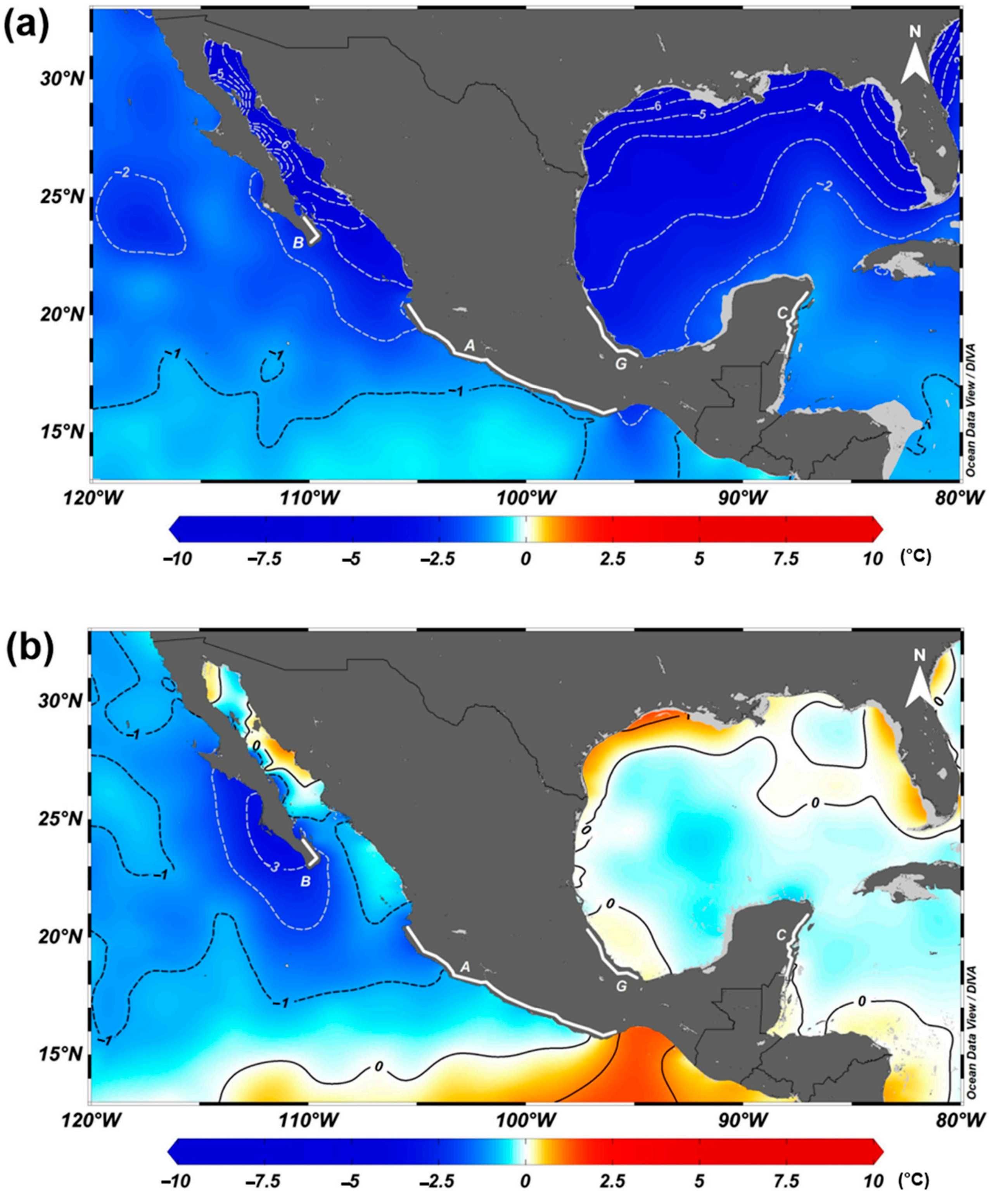

Figure 5. *Cont.*

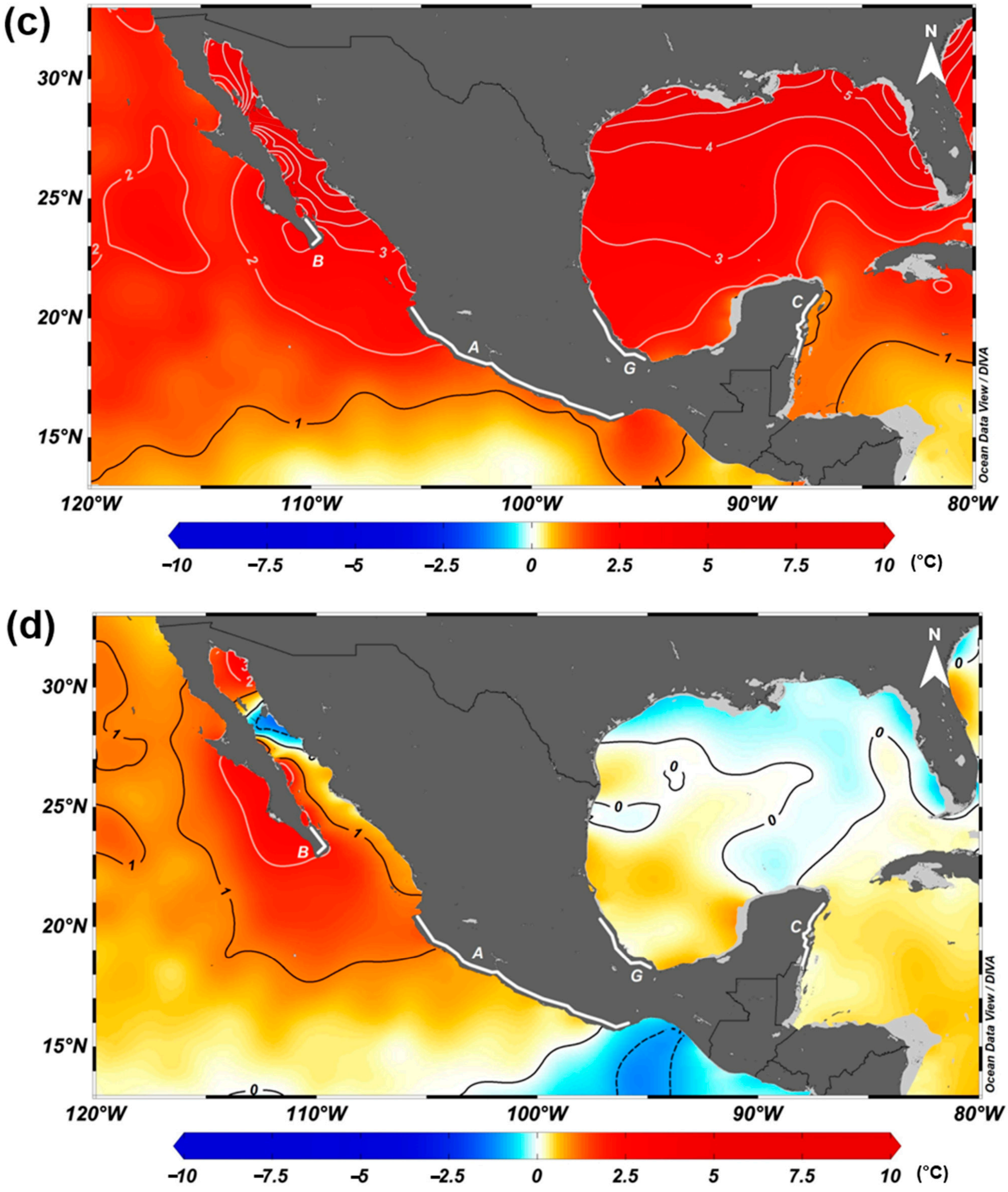

Figure 5. Seasonal ocean temperature (°C) minus annual climatology at a 10 m depth: (**a**) winter, (**b**) spring, (**c**) summer, and (**d**) autumn. The negative values indicate a trend beneath the annual average, while positive values indicate a trend over the annual average. The four zones of interest are shown with the white lines A, B, C, and G. WOA18 data.

Table 2. Temperature anomaly and latitude ranges: seasonal ocean temperature minus annual climatology at a 10 m depth.

Coast	SST10 Anomalies (°C)			
	Winter	Spring	Summer	Autumn
Pacific (A)	−2.5 to −1	−2 to 1	1 to 2.5	−0.6 to 1.5
Los Cabos (B)	−3 to −2	−3 to −2	2 to 3	1.5 to 2
Caribbean (C)	−2 to −1	−0.5 to 0	0 to 1.5	0 to 1
Gulf of Mexico (G)	−3 to −2	0 to 1	1.5 to 2.5	0 to 1

In the winter (Figure 5a), the anomalies everywhere attained negative values of between −3 and −1 °C in the oceanic domain, with much larger negative anomalies inside the Gulf of California and the northern Gulf of Mexico coastline. The South Pacific around line A had slightly negative anomalies but remained close to normal. In spring (Figure 5b), the Pacific (line A) was negative but close to normal, with the only positive anomalies in the south (up to 3 °C). Also, the Central Gulf of California and the coastal region of the Gulf of Mexico had positive values. The Caribbean, around line C, remained in normal spring values. By the summer (Figure 5c), the Pacific, around line A, showed anomalies from around 1 to 2 °C, while the Caribbean, around line C, had an anomaly of 1.5 °C. Los Cabos, near line B, was warmer (2 to 3 °C), similar to the Gulf of Mexico, near line G. In autumn (Figure 5d), the lowest anomaly was observed off Los Cabos (0.5 °C).

3.3.3. Seasonality of the Vertical Thermal Difference (VTD)

Figures 6 and 7 present the seasonal depths of the 20 °C and 18 °C VTD isotherms, respectively. These data were summarized for the areas of interest in Table 1. It was observed that the latitudinal depth gradient decreased toward the equator. In other words, the thermal resource will be found at more shallow depths at lower latitudes.

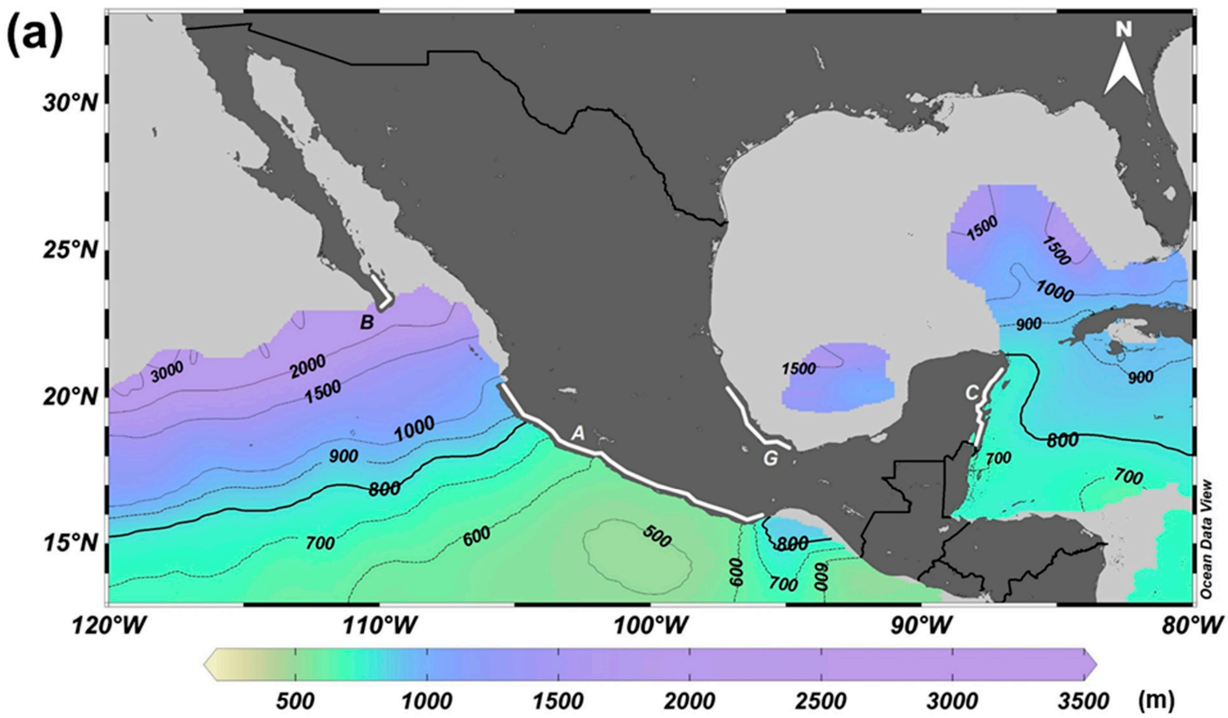

Figure 6. *Cont.*

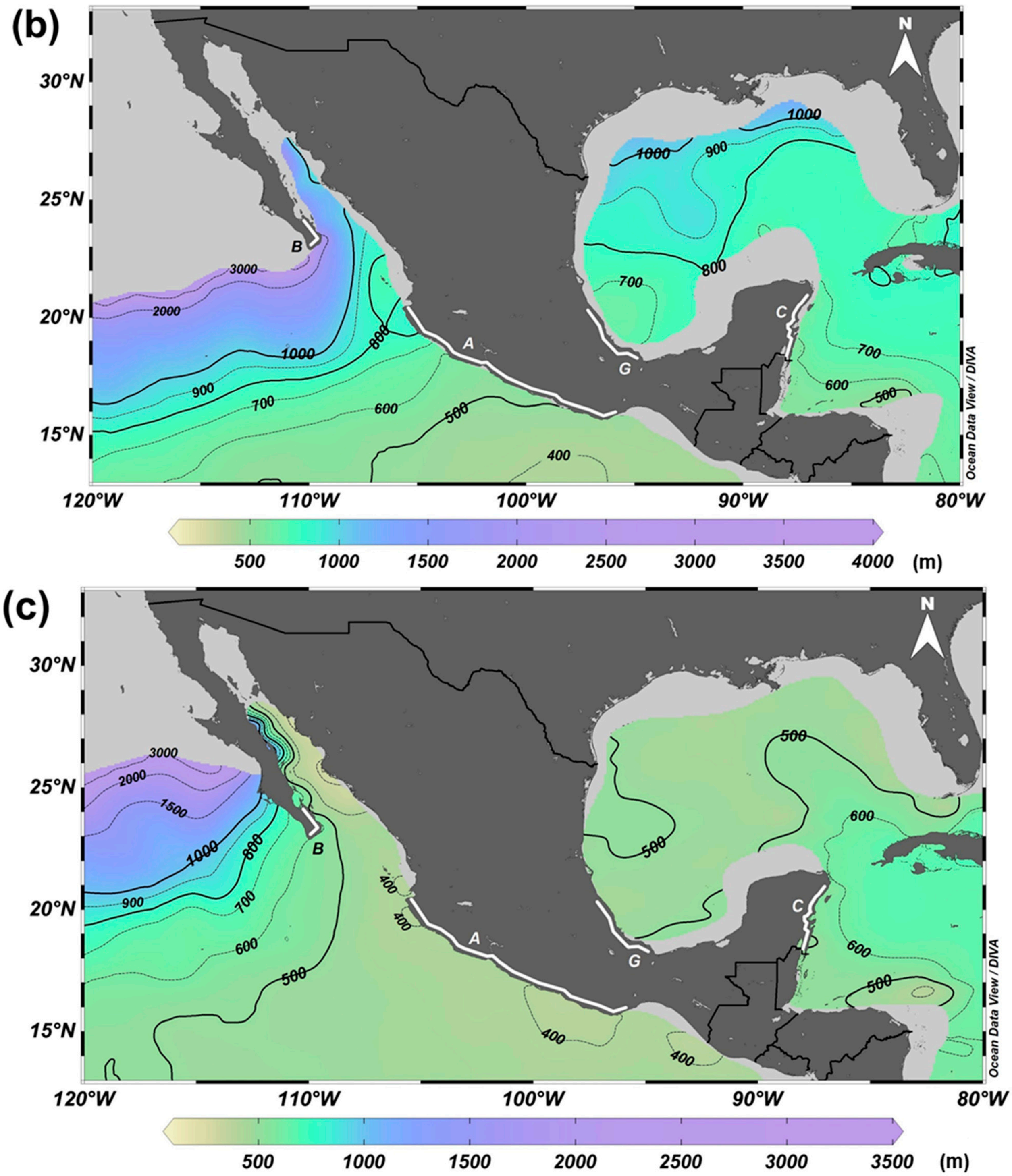

Figure 6. *Cont.*

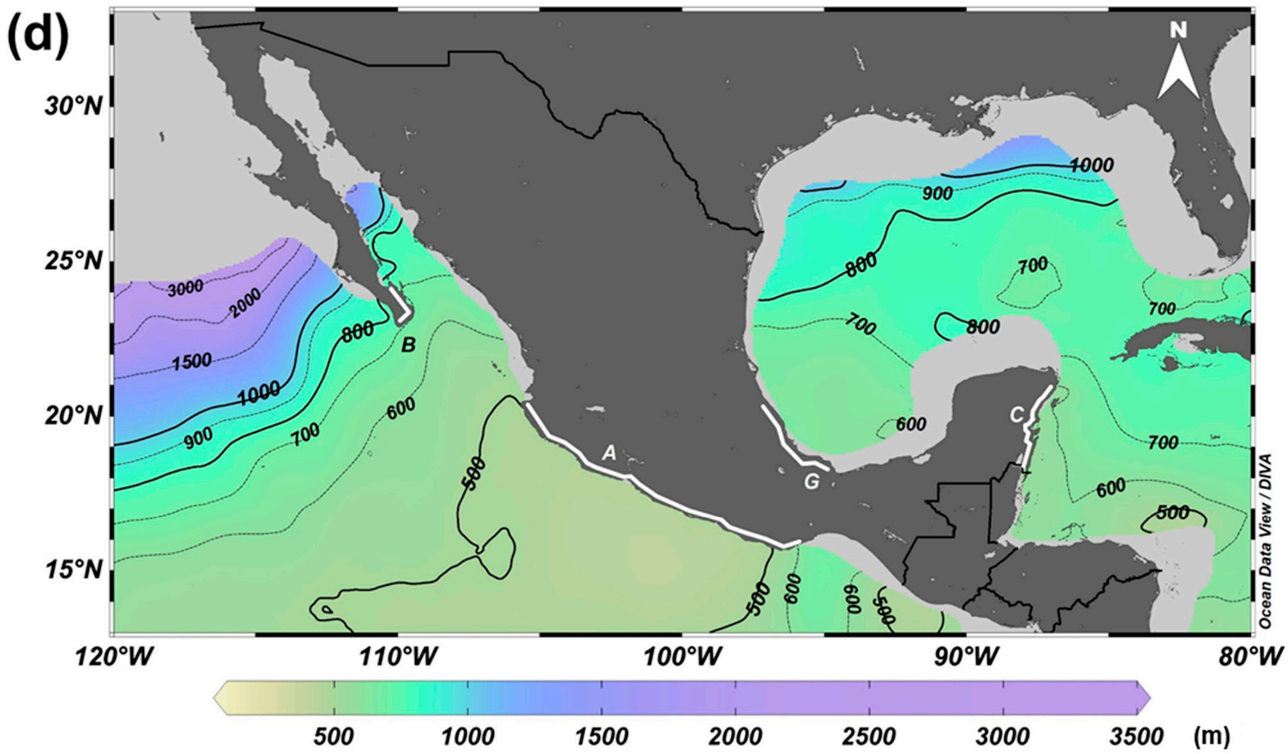

Figure 6. Seasonal depths of the 20 °C VTD isotherm, an optimal resource for OTEC plants: (**a**) winter, (**b**) spring, (**c**) summer, and (**d**) autumn. WOA18 data.

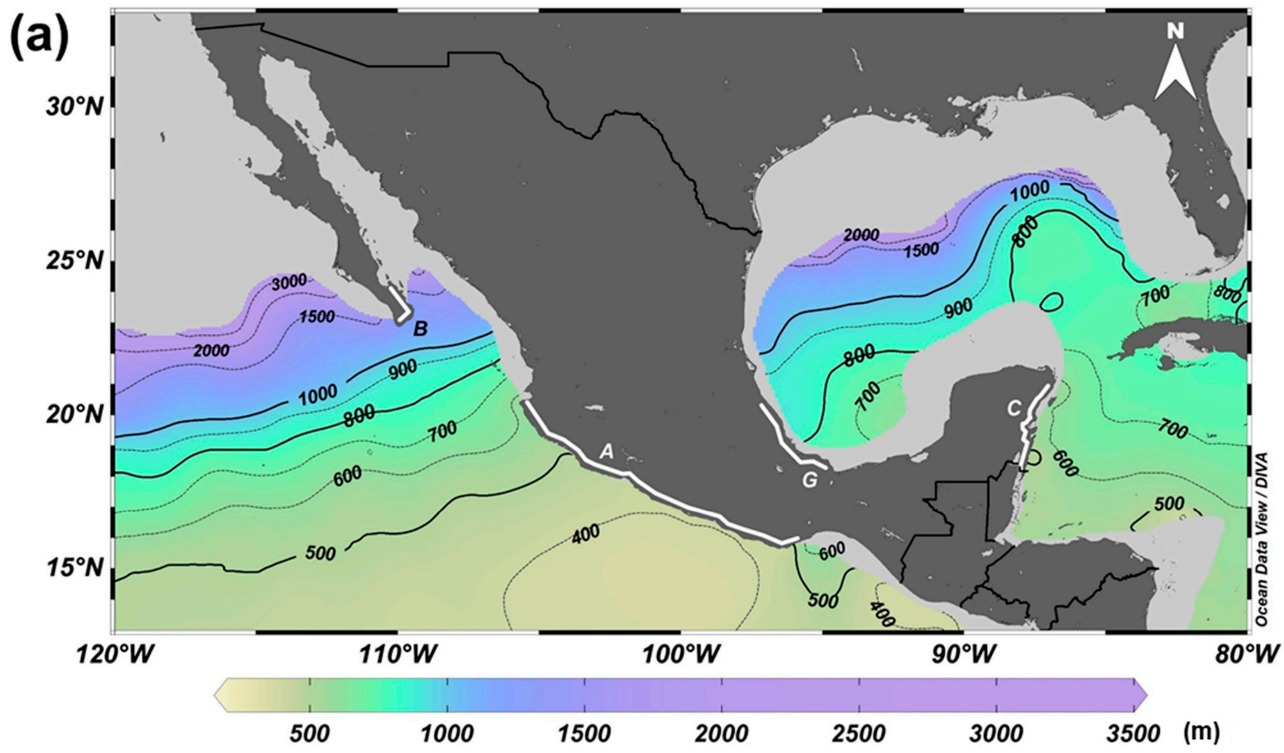

Figure 7. *Cont.*

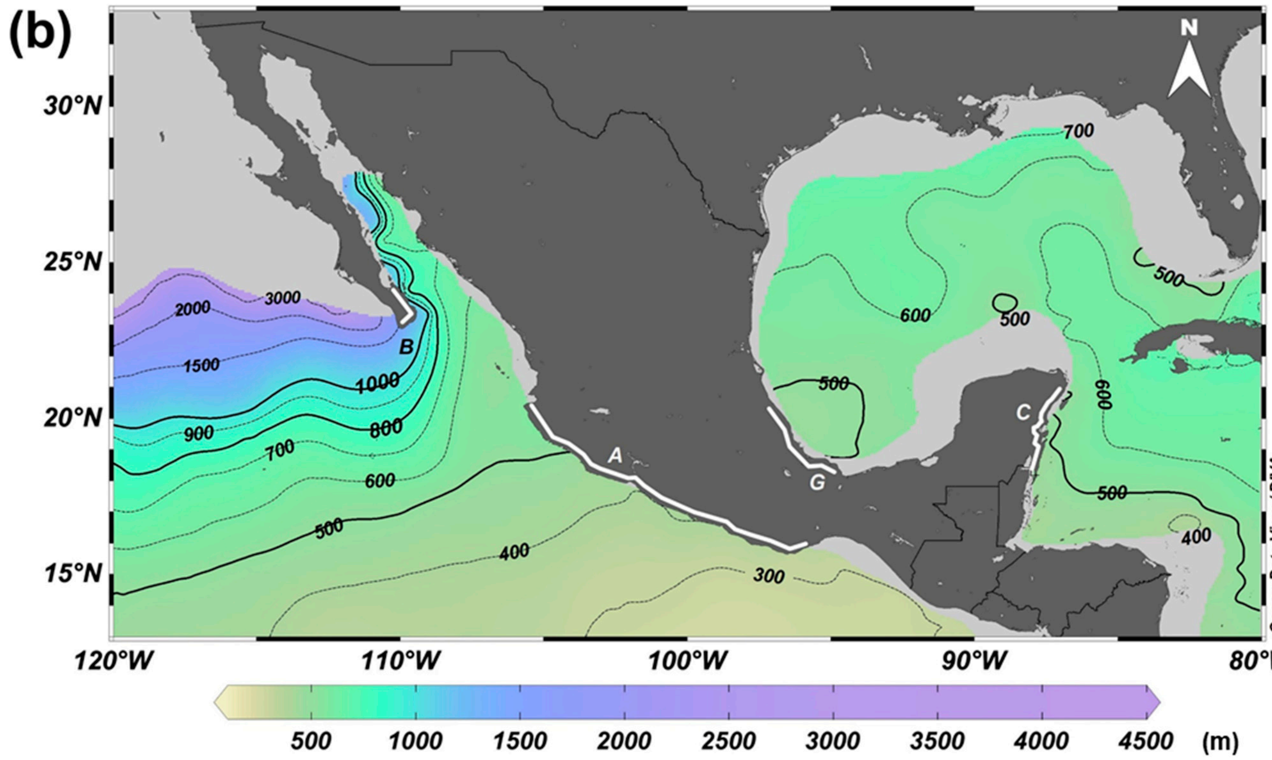

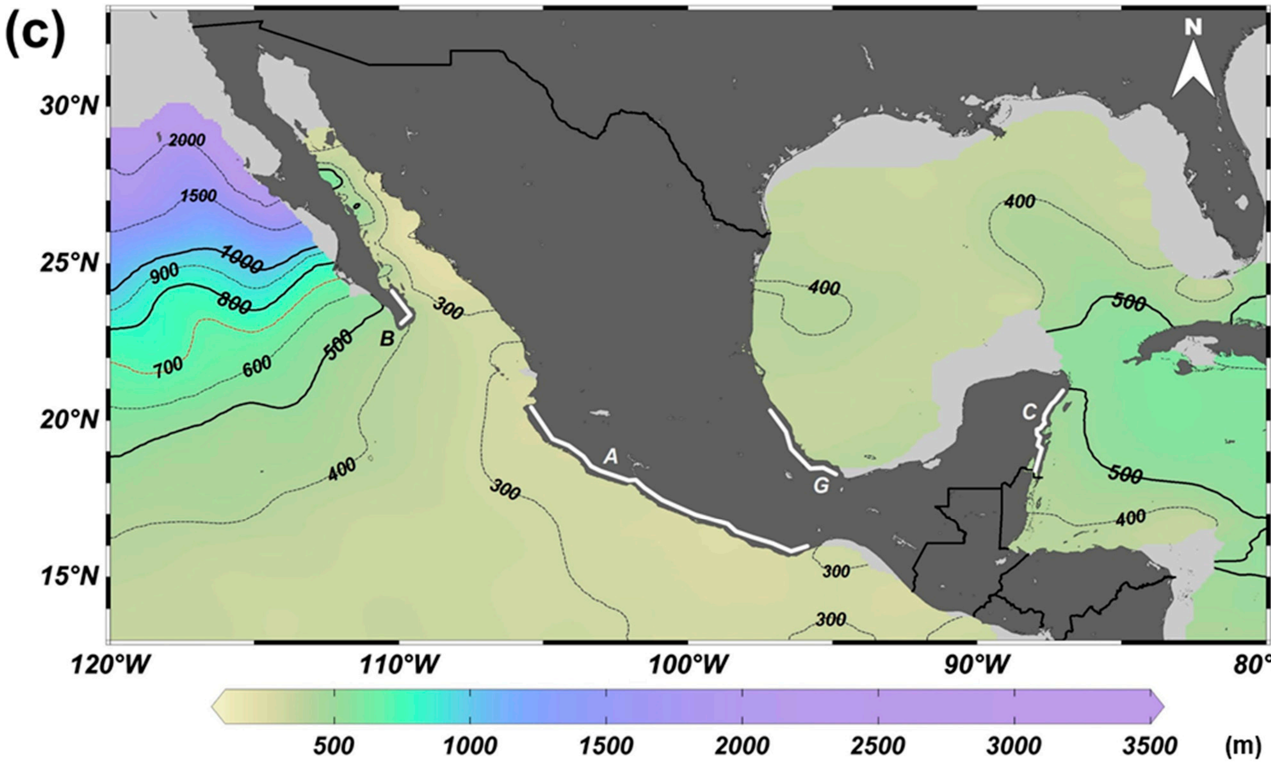

Figure 7. *Cont*.

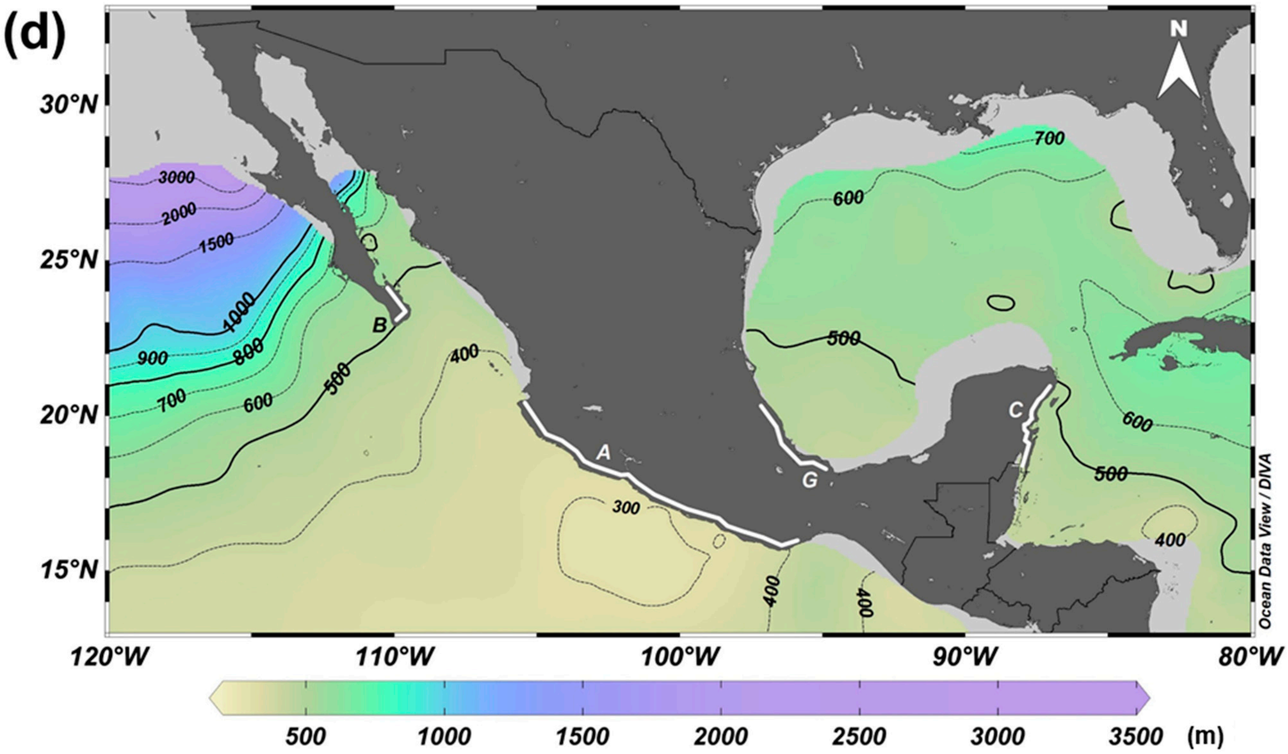

Figure 7. Seasonal depths of the suboptimal resource for the OTEC plant (18 °C VTD isotherm): (**a**) winter, (**b**) spring, (**c**) summer, and (**d**) autumn. WOA18 data.

4. Discussion

To determine VTD variations in Mexican oceanic waters, the annual and seasonal World Ocean Atlas [42] dataset was used, as field data were not available at a national scale in Mexico, and this free-access database contains hydrographic data of the world ocean on a regular grid, providing annual, seasonal, and monthly climatologies.

In designing an on-shore or off-shore OTEC plant, the coastal bathymetry is a critical factor, since the distance from the shore to the optimal temperature difference (VTD > 20 °C) must be less than 10 km, and suitable for a cold seawater pipeline to be laid. Four possible coastal areas were thus analyzed on the Mexican coasts (Figure 1).

OTEC technology requires huge quantities of water (in volume and mass) and a consistent source of hot or warm surface seawater (≥20 °C) and of cold seawater (≤5 °C), which are relatively clean of pollutants for 30 km around the site of the plant [1–4,23,41,49]. The average annual temperature indicated that water with a temperature greater than 23 °C was present in the four areas, at accessible depths of 20 to 130 m (Figure 2). Sea water with a temperature of less than 5 degrees was also present in the four areas, identified at accessible depths of 700 to 1000 m. The optimal annual average temperature difference (VTD ≥ 20 °C) for an OTEC plant was found in the four areas between 550 and 700 m (Figure 3b). Suboptimal conditions (18 ≤ VTD < 20 °C) were found in these areas at 440–750 m (Figure 3c). These findings generally agree with those of previous studies in Mexican waters [10,33–38,47,50].

The average temperature at a 10 m depth showed no water with optimal temperature in the winter in areas B and G, and in spring in area B. In addition, water with suboptimal temperature was absent during winter in area B (Figure 4).

The cold water at depths > 750 m did not present seasonal variation and its distribution was similar to that of the average annual temperature (<5 °C), indicating that the water at these depths was very stable, while the warmer water, at the surface, was influenced by seasonal changes in solar radiation and physical oceanographic processes.

The average annual temperature served as a reference point to find the seasonal temperature variability. The average temperature synthesized the variability that occurred during the period 1955–2017 and allowed us to estimate the trend of that variability through the temperature anomalies (Table 2 and Figure 5), which were between −3 and 3 °C throughout the year in the four analyzed areas. In winter, the anomalies had negative values (Table 2), indicating that the variation considered was normal, with respect to the average seasonal temperature, but highlighting the risk of not having optimal or suboptimal warm surface water in all the coastal areas examined (Figure 5a). In spring, the anomalies had negative values (Table 2), representing the risk of a lack of optimal or suboptimal surface water in the coastal areas A, B, and C (Figure 5b). In the summer and autumn, the anomalies presented positive values (Table 2), which indicated the presence of warm water with optimal and suboptimal conditions in the four coastal areas. The information suggests that major maintenance should be performed in winter on the entire OTEC plant, and that the plant should only be operational in summer and autumn, to avoid economic losses.

The optimal average seasonal VTD was not available in the areas B and G in the winter, nor was it available in area B during spring (Table 1 and Figure 6a,b). However, it was available in winter at accessible depths in the areas A and C (Table 1 and Figure 6a). During spring, it was accessible in areas A, C, and G (Table 1 and Figure 6b). During summer and autumn, the optimal thermal resource was found at accessible depths (Table 1 and Figure 6c,d) in the four areas.

Regarding the suboptimal average seasonal VTD, it was not available in area B in winter and spring, but it was accessible in summer and autumn at depths between 300 m and 500 m (Table 1 and Figure 7a,b). Furthermore, the suboptimal thermal resource was available during the four seasons of the year, and was accessible at depths between 350 m and 900 m in areas A, C, and G (Table 1 and Figure 7).

The results of our study are similar to the data found by Garduño Ruiz et al. [36], Garcia Huante [34], Garcia Huante et al. [35], Garduño Ruiz et al. [37], Chávez et al. [10], Alatorre et al. [33], Hernández Fontes et al. [38], and Acosta Pech et al. [50]. The slight differences may be a result of the seasons and timeframes used, and because the authors focused on specific points along the coast.

5. Conclusions

The results showed that there was only suitable cold, deep water accessible at depths of 800–1000 m throughout the year in the four areas identified. Warm surface water (SST10) at a 10 m depth was accessible in these areas, with an annual average of 24.7 °C in the Pacific and Los Cabos, 27.8 °C in the Caribbean, and 25.8 °C in the Gulf of Mexico. The surface temperature anomalies showed a seasonal variability of ±3 °C in the four areas: in winter, there were below-average values in all the areas, and in spring, values below the average occurred in the Pacific and Los Cabos areas. The seasonal variability of the required thermal resource suggested that the optimal temperature difference (VTD $\geq$ 20 °C) was available all year at depths of 400–1000 m in areas A and C, in area G in spring, summer, and autumn (9 months), and in area B in summer and autumn (6 months). In addition, the suboptimal temperature difference (18 $\leq$ VTD $<$ 20 °C) was available at depths of 350–800 m all year in areas A, C, and G. In B, this was only found in summer and autumn (6 months).

The design of an OTEC plant for any of the four areas must allow it to operate with surface water (SST10) of three degrees below the seasonal average value and a temperature difference greater than 23 °C. The cold-water intake must come from between 700 and 900 m depths to avoid seasonal variability of the surface water and ensure a temperature difference greater than 23 °C. Substantial maintenance of the plants must be carried out in winter and they must be operational throughout the entire year, with temperature differences greater than 18 °C in areas A, C, and G. Any plant in Los Cabos could only be operational during summer and autumn.

These results provide a useful guide of the seasonal variation in energy resources for OTEC implementation in four coastal areas in Mexico. However, they could also be extrapolated in any site of interest with similar characteristics (where the optimal or suboptimal thermal resource is found at depths of less than 1000 m) where OTEC deployment is being considered. Further monthly and local analyses are required to determine specific sites, along with an analysis of the technical potential, including energy production costs and environmental and social impact assessments.

Author Contributions: Conceptualization, C.M.C.-C., A.T.-C. and R.S.; methodology, C.M.C.-C.; validation, C.M.C.-C. and A.T.-C.; formal analysis, C.M.C.-C. and R.S.; investigation, C.M.C.-C., A.T.-C., V.C. and R.S.; resources, V.C. and R.S.; data curation, C.M.C.-C.; writing—original draft preparation, C.M.C.-C., A.T.-C., V.C. and R.S.; writing—review and editing, C.M.C.-C., A.T.-C., V.C. and R.S.; visualization, C.M.C.-C.; supervision, R.S.; project administration, V.C.; funding acquisition, R.S. All authors have read and agreed to the published version of the manuscript.

Funding: This work was supported by CONACYT–SENER–Sustentabilidad Energética, under grant FSE–2014–06–249795, "Centro Mexicano de Innovación en Energía del Océano (CEMIEOcéano)".

Institutional Review Board Statement: Not applicable.

Informed Consent Statement: Not applicable.

Data Availability Statement: The original contributions presented in the study are included in the article. Further inquiries can be directed to the corresponding authors.

Acknowledgments: We are thankful to the Grupos Interdisciplinarios de Investigación, Instituto de Ingeniería—UNAM, project "Sostenibilidad del Caribe mexicano: Cambiando debilidades en fortalezas", for the support to conduct this research.

Conflicts of Interest: The authors declare no conflicts of interest.

References

1. Anderson, J.H.; Anderson, J.H.J. History of Solar Power. Sea Solar Power Web Page. Available online: http://www.seasolarpower.com (accessed on 28 May 2024).
2. Uehara, H. The Present Status and Future of Ocean Thermal Energy Conversion (translated from Japanese). *Int. J. Sol. Energy* **1995**, *16*, 217–231. [CrossRef]
3. Claude, G. Power from the tropical seas. *Mech. Eng.* **1930**, *52*, 1039–1044.
4. Kalina, A.I. Generation of Energy by Means of a Working Fluid, and Regeneration of a Working Fluid. U.S. Patent 4,346,561 A, 31 August 1982.
5. Ascari, M.B.; Hanson, H.P.; Rauchenstein, L.; Van Zwieten, J.; Bharathan, D.; Heimiller, D.; Langle, N.; Scott, G.N.; Potemra, J.; Nagurny, N.J. *Ocean Thermal Extractable Energy Visualization-Final Technical Report on Award DE-EE0002664. October 28, 2012*; Lockheed Martin Mission Systems and Sensors: Syracuse, NY, USA, 2012.
6. Avery, W.H.; Wu, C. *Renewable Energy from the Ocean: A Guide to OTEC*; Oxford University Press: Oxford, UK, 1994.
7. Rajagopalan, K.; Nihous, G.C. Estimates of global Ocean Thermal Energy Conversion (OTEC) resources using an ocean general circulation model. *Renew. Energy* **2013**, *50*, 532–540. [CrossRef]
8. Aresti, L.; Christodoulides, P.; Michailides, C.; Onoufriou, T. Reviewing the energy, environment, and economy prospects of Ocean Thermal Energy Conversion (OTEC) systems. *Sustain. Energy Technol. Assess.* **2023**, *60*, 103459. [CrossRef]
9. Wolff, W. *OTEC Thermal Resource Report for Caribbean Sea Plant Ship 13–15/sup 0/N 75–80/sup 0/N*; Ocean Data Systems, Inc.: Monterey, CA, USA, 1979.
10. Chávez, V.; Bárcenas, J.F.; Martínez, M.L.; Mateos, E.; Zúñiga-Ríos, A.; Guimarais, M.; Wojtarowski, A.; Landgrave, R.; Ceballos Canché, C.H.; Silva, R. Potential sites for the use of ocean energy in the Mexican Caribbean. *Energy Sources Part B Econ. Plan. Policy* **2023**, *18*, 2160524. [CrossRef]
11. Frye, D.; Davison, A. *Physical Oceanographic Data from the OTEC Punta Tuna, Puerto Rico Site: September 1979–June 1980*; Lawrence Berkeley Laboratory: Berkeley, CA, USA, 1981.
12. Lee, T.N.; Munier, R.S.; Chiu, S. *Water Mass Structure and Variability North of St. Croix, US Virgin Islands, as Observed during the Summer of 1977 for OTEC Assessment*; University of Miami: Coral Gables, FL, USA, 1978.
13. McGowan, J.G.; Heronemus, W.E. Gulf-Stream-Based, Ocean-Thermal Power Plants. *J. Hydronautics* **1976**, *10*, 33–38. [CrossRef]
14. Rauchenstein, L. Global Distribution of Ocean Thermal Energy Conversion (OTEC) Resources and Applicability in U.S. Waters Near Florida. Master's Thesis, Florida Atlantic University, Boca Raton, FL, USA, 2012.
15. Leland, A.E. A Resource Assessment of Southeast Florida as Related to Ocean Thermal Energy. Master's Thesis, Florida Atlantic University, Boca Raton, FL, USA, 2009.

16. Mangarella, P.A.; Heronemus, W.E. Thermal properties of the Florida current as related to ocean thermal energy conversion (OTEC). *Sol. Energy* **1979**, *22*, 527–533. [CrossRef]
17. Wolff, P.; Levit, H.; Steuckert, J.; Wolff, W. *OTEC Thermal Resource Report for Central Gulf of Mexico. Prepared for the US Department of Energy under Contract No. EC-77-C-O1-4028*; Ocean Data Systems, Inc.: Monterey, CA, USA, 1977.
18. Neto, A.G.; Hiron, L.; Pimenta, F.M.; Rodrigues, R.R. Northeast Brazil potential for land-based OTEC implementation. In Proceedings of the 2014 Ninth International Conference on Ecological Vehicles and Renewable Energies (EVER), Monte-Carlo, Monaco, 25–27 March 2014; pp. 1–4.
19. Wolff, W.A. *OTEC Thermal Resource Report for Ivory Coast*; Ocean Data Systems, Inc.: Monterey, CA, USA, 1979.
20. Kim, H.-J.; Lee, H.-S.; Lim, S.-T.; Petterson, M. The suitability of the pacific islands for harnessing ocean thermal energy and the feasibility of OTEC plants for onshore or offshore processing. *Geosciences* **2021**, *11*, 407. [CrossRef]
21. Wolff, W. *OTEC Thermal Resource Report for Pacific Plant Ship 5–10 Degrees N 90–95 Degrees W*; Ocean Data Systems, Inc.: Monterey, CA, USA, 1979.
22. Wolff, W.A. *OTEC Thermal Resource Report for Dampier Land, Australia. HCP/T2898-01/6*; Ocean Data Systems, Inc.: Monterey, CA, USA, 1979.
23. Uehara, H.; Dilao, C.O.; Nakaoka, T. Conceptual design of ocean thermal energy conversion (OTEC) power plants in the Philippines. *Sol. Energy* **1988**, *41*, 431–441. [CrossRef]
24. Owens, W.L.; Trimble, L.C. Mini-OTEC operational results. *J. Sol. Energy Eng.* **1981**, *103*, 233–240. [CrossRef]
25. Waid, R. The mini-OTEC test. In Proceedings of the OCEANS'79, San Diego, CA, USA, 17–19 September 1979; pp. 548–552.
26. Wolff, W.A. *OTEC Thermal Resource Report for Guam*; Ocean Data Systems, Inc.: Monterey, CA, USA, 1979.
27. Wolff, W.A. *OTEC Thermal Resource Report for Manila, Philippine Islands. HCP/T2898-01/8*; Ocean Data Systems, Inc.: Monterey, CA, USA, 1979.
28. Petterson, M.G.; Kim, H.J. Can Ocean Thermal Energy Conversion and Seawater Utilisation Assist Small Island Developing States? A Case Study of Kiribati, Pacific Islands Region. In *Ocean Thermal Energy Conversion (OTEC)*; Albert, S.K., Hyeon-Ju, K., Eds.; IntechOpen: Rijeka, Croatia, 2020; Chapter 1.
29. Fouzi, A.; Hooi-Siang, K.; Omar, Y.; Muhammad Noor Afiq Witri Muhammad, Y. Review of Resources from the Perspective of Wave, Tidal, and Ocean Thermal Energy Conversion. *J. Adv. Res. Appl. Sci. Eng. Technol.* **2023**, *30*, 127–149. [CrossRef]
30. Wolff, W.A. *OTEC Thermal Resource Report for Sri Lanka (No. HCP/T2898-01/2)*; Ocean Data Systems, Inc.: Monterey, CA, USA, 1979.
31. Wolff, W.A. *OTEC Thermal Resource Report for Mombasa*; Ocean Data Systems, Inc.: Monterey, CA, USA, 1979.
32. Wolff, W.A. *OTEC Thermal Resource Report for Jakarta, Indonesia*; Ocean Data Systems, Inc.: Monterey, CA, USA, 1979.
33. Alatorre, M.; Garcia, A.; Cerezo, E.; Barcenas, F.; Jimenez, A.; Silva, R. OTEC instalation posibilities in Mexico. In Proceedings of the 5th OTEC Symposium, Saint Pierre, France, 7–9 November 2017.
34. García Huante, A.; Rodríguez Cueto, Y.; Hernández Contreras, R.E.; Garduño Ruíz, E.P.; Alatorre Mendieta, M.Á.; Silva, R. Validation of Sea-Surface Temperature Data for Potential OTEC Deployment in the Mexican Pacific. *Energies* **2021**, *14*, 1898. [CrossRef]
35. García Huante, A.; Rodríguez Cueto, Y.; Silva, R.; Mendoza, E.; Vega, L.A. Determination of the potential thermal gradient for the Mexican Pacific Ocean. *J. Mar. Sci. Eng.* **2018**, *6*, 20. [CrossRef]
36. Garduño Ruiz, E.P.; García Huante, A.; Rodríguez Cueto, Y.; Bárcenas Graniel, J.F.; Alatorre Mendieta, M.Á.; Cerezo Acevedo, E.; Tobal Cupul, J.G.; Romero Medina, V.M.; Silva Casarín, R. *Conversión de Energía Térmica Oceánica (OTEC) Estado del Arte*; Cemie-Océano, Universidad Autónoma de Campeche: Campeche, Mexico, 2017; 123p.
37. Garduño-Ruiz, E.P.; Silva, R.; Rodríguez-Cueto, Y.; García-Huante, A.; Olmedo-González, J.; Martínez, M.L.; Wojtarowski, A.; Martell-Dubois, R.; Cerdeira-Estrada, S. Criteria for optimal site selection for ocean thermal energy conversion (Otec) plants in Mexico. *Energies* **2021**, *14*, 2121. [CrossRef]
38. Hernández-Fontes, J.V.; Felix, A.; Mendoza, E.; Cueto, Y.R.; Silva, R. On the marine energy resources of Mexico. *J. Mar. Sci. Eng.* **2019**, *7*, 191. [CrossRef]
39. Macías-Carballo, M.; Torres-Navarrete, C.R.; Larios-Castillo, S.I.; Ramos-Hernández, R.; García-Toscano, J. *Atlas Oceanográfico de las Costas de la Península de Baja California*; Universidad Autónoma de Baja California: Mexicali, Mexico, 2013; 228p.
40. Wolff, W.A. *OTEC Thermal Resource Report for Western Coast Mexico*; Ocean Data Systems, Inc.: Monterey, CA, USA, 1979.
41. Morisaki, T.; Yasunaga, T.; Ikegami, Y. Potential Evaluation of Ocean Thermal Energy Conversion. *J. OTEC* **2015**, *20*, 21–31. (In Japanese)
42. WOA18. World Ocean Atlas 2018. Available online: http://www.nodc.noaa.gov/cgi%E2%80%93bin/OC5/woa18/woa18.pl (accessed on 6 June 2024).
43. GEBCO. General Bathymetric Chart of the Ocean. Available online: https://www.gebco.net/ (accessed on 4 June 2024).
44. Vega, L.A. Economics of Ocean Thermal Energy Conversion (OTEC): An Update. In Proceedings of the Offshore Technology Conference, Houston, TX, USA, 3–6 May 2010; p. OTC-21016-MS.
45. Cerdeira-Estrada, S.; López-Saldaña, G. A novel Satellite-based Ocean Monitoring System for Mexico. *Cienc. Mar.* **2011**, *37*, 237–247. [CrossRef]
46. Boyer, T.P.; Baranova, O.K.; Coleman, C.; Garcia, H.E.; Grodsky, A.; Locarnini, R.A.; Mishonov, A.V.; Paver, C.R.; Reagan, J.R.; Seidov, D.; et al. *World Ocean Database 2018*; NOAA Atlas NESDIS 87; Mishonov, A.V., Ed.; Ocean Climate Laboratory: Silver Spring, MD, USA, 2018.

47. Garcia, H.E.; Boyer, T.P.; Baranova, O.K.; Locarnini, R.A.; Mishonov, A.V.; Grodsky, A.; Paver, C.R.; Weathers, K.W.; Smolyar, I.V.; Reagan, J.R.; et al. *World Ocean Atlas 2018: Product Documentation*; Mishonov, A., Ed.; Ocean Climate Laboratory: Silver Spring, MD, USA, 2019. Available online: https://data.nodc.noaa.gov/woa/WOA18/DOC/woa18documentation.pdf (accessed on 6 June 2024).
48. Locarnini, M.; Mishonov, A.; Baranova, O.; Boyer, T.; Zweng, M.; Garcia, H.; Seidov, D.; Weathers, K.; Paver, C.; Smolyar, I. *World Ocean Atlas 2018, Volume 1: Temperature*; NOAA Atlas NESDIS 81; Mishonov, A., Ed.; Ocean Climate Laboratory: Silver Spring, MD, USA, 2018; 52p.
49. Anderson, J.H. A Proposal for a New Application of Thermal Energy from the Sea. Bachelor's Thesis, Massachusetts Institute of Technology, Cambridge, MA, USA, 1963.
50. Acosta-Pech, I.d.J.; Ovando Sierra, J.C.; Andrade Duran, J.E.; Castillo Télles, M. Potencial de Energía Térmica en el Golfo de México. *Rev. Energía Química Física* **2017**, *4*, 14–27.

Disclaimer/Publisher's Note: The statements, opinions and data contained in all publications are solely those of the individual author(s) and contributor(s) and not of MDPI and/or the editor(s). MDPI and/or the editor(s) disclaim responsibility for any injury to people or property resulting from any ideas, methods, instructions or products referred to in the content.